

Interfacial effects on the tunneling magnetoresistance in $\text{La}_{0.7}\text{Sr}_{0.3}\text{MnO}_3/\text{MgO}/\text{Fe}$ tunneling junctions

R. Galceran,¹ Ll. Balcells,¹ C. Martínez-Boubeta,^{2,*} B. Bozzo,¹ J. Cisneros-Fernández,¹ M. de la Mata,¹ C. Magén,³ J. Arbiol,^{1,4} J. Tornos,⁵ F. A. Cuellar,⁵ Z. Sefrioui,⁵ A. Cebollada,⁶ F. Golmar,^{7,8} L. E. Hueso,^{8,9} F. Casanova,^{8,9} J. Santamaría,⁵ and B. Martínez¹

¹*Instituto de Ciencia de Materiales de Barcelona (ICMAB-CSIC), Campus UAB, Bellaterra 08193, Spain*

²*University of Barcelona, 08007 Barcelona, Spain*

³*Laboratorio de Microscopías Avanzadas (LMA), Instituto de Nanociencia de Aragón (INA) - ARAID, and Departamento de Física de la Materia Condensada, Universidad de Zaragoza, 50018 Zaragoza, Spain*

⁴*Institució Catalana de Recerca i Estudis Avançats (ICREA), 08010 Barcelona, Spain*

⁵*Grupo de Física de Materia Condensada (GFMC), Departamento Física Aplicada III, F. de Física, Universidad Complutense, 28040 Madrid, Spain*

⁶*Instituto de Microelectrónica de Madrid (IMM-CNM-CSIC), Isaac Newton 8, PTM, 28760 Tres Cantos, Spain*

⁷*Consejo Nacional de Investigaciones Científicas y Técnicas- Instituto Nacional de Tecnología Industrial (CONICET-INTI) and Escuela de Ciencia y Tecnología - Universidad Nacional de San Martín (ECyT-UNSAM), San Martín, Bs. As., Argentina*

⁸*CIC nanoGUNE, 20018 Donostia-San Sebastian, Basque Country, Spain*

⁹*IKERBASQUE, Basque Foundation for Science, 48011 Bilbao, Basque Country, Spain*

(Received 12 March 2015; revised manuscript received 18 June 2015; published 16 September 2015)

We report on magnetotransport properties on $\text{La}_{0.7}\text{Sr}_{0.3}\text{MnO}_3/\text{MgO}/\text{Fe}$ tunnel junctions grown epitaxially on top of (001)-oriented SrTiO_3 substrates by sputtering. It is shown that the magnetoresistive response depends critically on the MgO/Fe interfacial properties. The appearance of an FeO_x layer by the interface destroys the Δ_1 symmetry filtering effect of the MgO/Fe system and only a small negative tunneling magnetoresistance (TMR) ($\sim -3\%$) is measured. However, in annealed samples a switchover from positive TMR ($\sim +25\%$ at 70 K) to negative TMR ($\sim -1\%$) is observed around 120 K. This change is associated with the transition from semiconducting at high T to insulating at low T taking place at the Verwey transition ($T_V \sim 120$ K) in Fe_3O_4 , thus suggesting the formation of a very thin slab of magnetite at the MgO/Fe interface during annealing treatments. These results highlight the relevance of interfacial properties on the tunneling conduction process and how it can be substantially modified through appropriate interface engineering.

DOI: [10.1103/PhysRevB.92.094428](https://doi.org/10.1103/PhysRevB.92.094428)

PACS number(s): 73.50.-h, 73.63.-b, 75.47.-m, 73.40.Rw

I. INTRODUCTION

Magnetic tunnel junctions (MTJs) consist of two ferromagnetic (FM) electrodes separated by a thin insulating barrier. The relative conductance variation by flipping the magnetization between the parallel and antiparallel alignments of those electrodes is called tunneling magnetoresistance (TMR). According to Jullière's model, its value is given by $2PP'/(1 + PP')$, P and P' being the tunneling electron spin polarizations of the junction's two electrode/barrier interfaces [1]. Therefore, in the search for improving TMR response, half-metallic ferromagnets are one of the most suitable materials because they provide full spin polarization at the Fermi level. Among those materials manganites such as $\text{La}_{0.7}\text{Sr}_{0.3}\text{MnO}_3$ (LSMO) have been intensively investigated [2]; however, their performances are drastically reduced at room temperature (RT) and other half-metallic materials, such as Co-based Heusler alloys with Curie temperatures well above RT [3], have become the topic of interest in the past few years. Besides full spin polarization, half metals also provide full symmetry polarization of current, which allows studying the symmetry filtering effect across MgO barriers [4]. On the other hand, it is well known that the tunneling process also depends critically on the electronic structure of the barrier and on the microscopic

features at the electrode/barrier interfaces. Thus, acting on these aspects through interface engineering may become a very appealing procedure for improving TMR response [5,6]. High polarization can also be achieved by choosing an appropriate electrode/barrier combination, as in the case of MTJ with epitaxial Fe (001) electrodes and MgO barriers [7], where the coherent (spin and symmetry conserving) tunneling process promotes the predominant transmission of electronic states with Δ_1 character with the majority spin orientation, resulting in giant TMR values exceeding 100% [8,9].

In this scenario, the use of transition-metal oxides in MTJs may be the source of a plethora of interesting new phenomena resulting from the combined effect of electron correlations with various possible forms of symmetry breaking at the interfaces [6]. An example is the case of the $\text{LaMnO}_3/\text{SrMnO}_3$ interface, where interface engineering encompasses modifications in orbital occupancy, which give rise to the appearance of ferromagnetism at the interface between these two antiferromagnets (AF) [10]. Moreover, modified bonding at the interface can cause interesting spin-filtering effects responsible for nonmonotonic and highly anomalous dependences of the TMR response with temperature or applied bias [11]. In particular, the combination of perovskite manganites with MgO barriers may yield interesting effects resulting from the different lattice structures and from the high degree of epitaxial strain in this interface. In fact, high-field MR values above 500% have been already reported in the LSMO/ MgO/Fe system,

*Present address: Santiago de Compostela, Spain.

although the effect cannot be linked to the rotation of the magnetic electrodes [12]. However, the Fe/MgO combination may also introduce spin depolarization due to the formation of nonstoichiometric Fe oxides, as recently shown both experimentally and theoretically, drastically reducing TMR values [13]. Of particular interest is the formation of magnetite (Fe_3O_4), which shows a high spin polarization at the Fermi level as well as a high Curie temperature, $T_C \sim 585^\circ\text{C}$. In addition, magnetite exhibits a transition from semiconducting at high temperature to insulating at low temperature at the Verwey temperature $T_V \sim 120\text{ K}$, [14] which may have a strong influence on the tunneling conduction process.

In this work we report on the magnetotransport properties of magnetic tunnel junctions made from highly epitaxial LSMO (42 nm)/MgO/Fe (20 nm) heterostructures grown on top of TiO_2 -terminated (100) SrTiO_3 (STO) substrates by magnetron sputtering, as described elsewhere [15]. Samples exhibit a negative TMR response of about 3% at 100 K, which indicates that the Δ_1 symmetry filtering effect expected for the MgO/Fe system has been suppressed. Interestingly, annealing treatment (400°C for half hour in high vacuum) allows obtaining a positive TMR response with values of $\sim 25\%$ at 70 K and pronounced dependence on the voltage bias. However, the positive TMR response vanishes at $T \sim 120\text{ K}$ and, for higher temperatures only the small ($\sim 1\%$) negative TMR response is found. This behavior is explained in terms of the existence of an iron oxide layer at the MgO/Fe interface with an important effect on the electronic structure of the interface and on the tunneling conduction process. In fact, scanning transmission electron microscope (STEM) pictures show a blurred Fe/MgO interface, suggesting the presence of FeO_x irregularly distributed at this interface. Annealing substantially modifies the structural quality and oxygen content of this interfacial oxide, as demonstrated by x-ray photoelectron spectroscopy (XPS), promoting the formation of a very thin continuous FeO_x layer. The change of the TMR sign at $T \sim 120\text{ K}$, i.e., in accordance with the Verwey transition temperature of Fe_3O_4 , strongly suggests the formation of magnetite during the annealing process. Thus the observed positive TMR would be explained in terms of the interplay between the complex band structure of transition-metal oxides and different electronic symmetries similar to those discussed in Ref. [4]. The effect of the MgO barrier thickness on the TMR response has also been analyzed, making evident that for thin enough barriers electrodes are antiferromagnetically coupled. These results evidence once more the relevance of interfacial properties on the final performances of MTJs and highlight the promising role of interface engineering to obtain devices with new and enhanced functionalities.

II. EXPERIMENTAL

LSMO/MgO bilayers were grown by magnetron sputtering in oxygen plasma at 900°C and 600°C , respectively. Then the sample was transferred to another vacuum chamber for growth of the Fe layer. Prior to Fe deposition, the bilayers were annealed (to suppress surface hydroxylation due to air exposure) for 30 min at 400°C . The Fe layers were protected with Ti and Au capping layers. Samples with different MgO barrier thicknesses ($t = 1.2$ and 2.4 nm) were prepared and

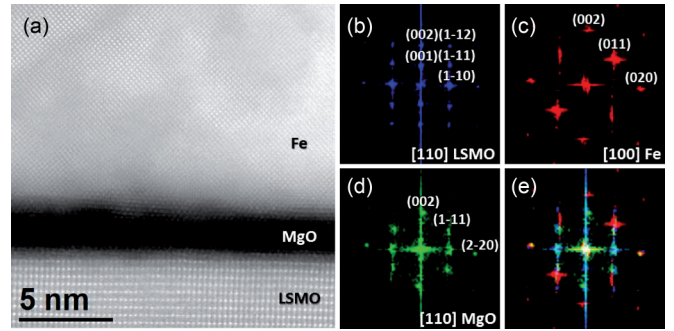


FIG. 1. (Color online) (a) HAADF-STEM image of a cross section of a postannealed $\text{La}_{0.7}\text{Sr}_{0.3}\text{MnO}_3/\text{MgO}/\text{Fe}$ heterostructure evidencing the crystallinity of the different layers. However, the MgO/Fe interface is blurred and rough evidencing some structural disorder. (right) Power spectra obtained on the different layers forming the heterostructure: (b, blue) LSMO, (c, red) Fe, and (d, green) MgO. (e) The RGB power spectra contains the previous spectra overlapped showing their epitaxial relationship.

up to eight rectangular-shaped junction pillars were patterned on each sample by using optical lithography and Ar-ion milling [6], their areas ranging from 2×4 to $18 \times 9\ \mu\text{m}^2$ (see Fig. S1 from Supplemental Material [16]). Transport measurements were done using a Keithley source in the dc two-probe configuration, with positive bias corresponding to the electrons tunneling from the top Fe electrode to the bottom LSMO electrode. Magnetic measurements were performed by applying the magnetic field (H) parallel to the sample surface. In-plane measurements were done along the [100] Fe easy axis, which coincides with the [110] axis of MgO, LSMO, and STO, and also the long side of the patterned rectangles. (See sketch of the configuration in Fig. S1 and in-plane anisotropy measurements in Fig. S4 from the Supplemental Material [16].) Both field and temperature were carefully controlled in a Quantum Design physical property measurement system (PPMS).

Microstructural characterization of the heterostructures, by using high-angle annular dark-field scanning transmission electron microscopy (HAADF-STEM) was carried out in a probe-corrected FEI Titan 60–300 operated at 300 kV with a probe size below $1\ \text{\AA}$. The local structure of the multilayer can be appreciated from the HAADF-STEM image shown in Fig. 1 (left), in which the high crystallinity of the layers is apparent. Whereas the bottom LSMO/MgO interface is abrupt, the top MgO/Fe interface is blurred and rough, thus evidencing some structural disorder due to the detrimental effect of air exposure on the topmost MgO atomic layers during the transferring of samples for Fe deposition. Power spectra obtained on the different regions of the heterostructure confirm the epitaxial relationship between the different layers of materials [see Fig. 1 (right side)], although a rotation of 2° – 4° of the MgO layer with respect to the LSMO layer is detected.

III. RESULTS AND DISCUSSION

The blurred Fe/MgO interface observed in STEM experiments (see Fig. 1) suggests the existence of some structural disorder at this interface which would promote the formation

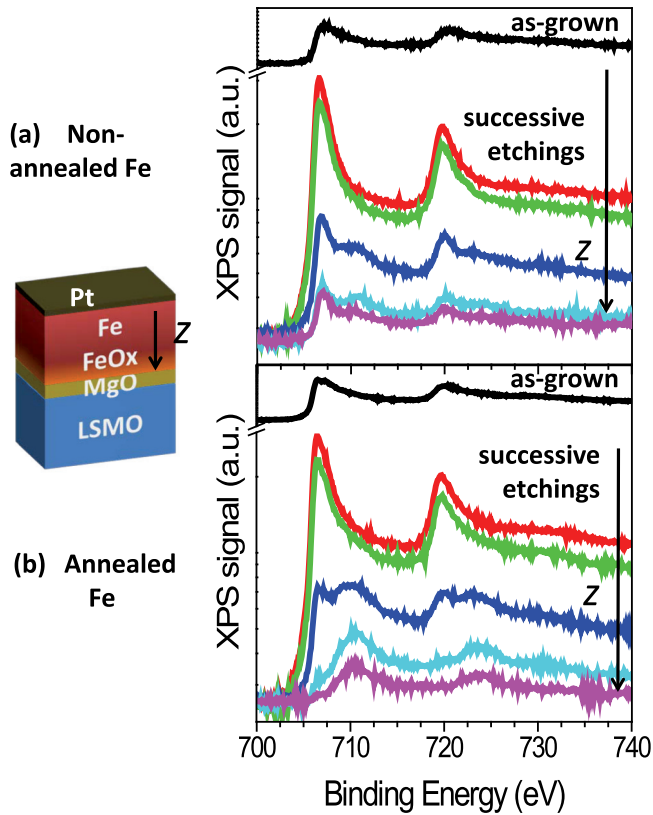


FIG. 2. (Color online) XPS spectra in the Fe $2p$ region of a Pt/Fe/MgO/La_{0.7}Sr_{0.3}MnO₃/STO stack for different sample preparation conditions: (a) Fe grown with no *in situ* annealing after deposition and (b) Fe grown with an *in situ* annealing at 400 °C for 30 min after the deposition.

of iron oxide (FeO_x), thus playing an important role in the behavior displayed by the junctions. The relevance of the microstructure of the MgO/Fe interface has been clearly pointed out in the literature [8,17–23]. The existence of FeO_x at the interface has been reported in several cases, showing that its amount depends critically on the MgO growth method. FeO_x has been shown to form at the interface between Fe and MgO due to Fe-O bonding [24]. The detrimental effect of this FeO_x layer on the TMR response, and its improvement after different thermal annealing treatments, has also been previously reported [25]. To suppress or reduce as much as possible the formation of this FeO_x layer, we have analyzed different strategies. We have considered the growth of the Fe layer in a reductive atmosphere (95% Ar + 5% H₂), however this results in a substantial reduction of the LSMO Curie temperature ($T_C \sim 250$ K), in spite of the LSMO layer being capped with the MgO barrier. Next we checked the effectiveness of an annealing process (400 °C for 30 min at high vacuum after Fe layer deposition). XPS analysis of the Fe $2p$ and Mg $1s$ regions of the whole Pt/Fe/MgO/LSMO/STO heterostructure reveals the presence of FeO_x close to the Fe/MgO interface (see Figs. 2 and S2 in the Supplemental Material). Interestingly enough, the peak at binding energy of about 710 eV, which would indicate the presence of FeO_x (Fe²⁺ and Fe³⁺), is more intense in the annealed sample, thus indicating an enhancement of the FeO_x layer after annealing.

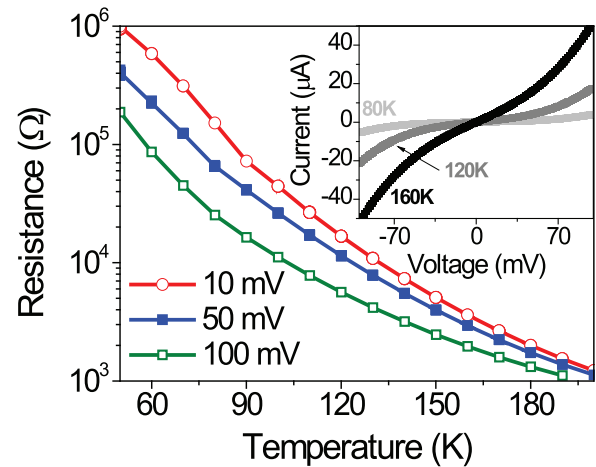


FIG. 3. (Color online) Temperature dependence of the resistance of the LSMO/MgO/Fe annealed junctions in the low- T regime for different voltage bias values. Inset shows nonlinear I - V curves obtained for different temperatures (80, 120, and 160 K).

This result is contrary to the tendency usually reported for MgO/Fe interfaces in Fe/MgO/Fe heterostructures, thus suggesting that the LSMO layer may well act as an extra source of oxygen for the oxidation of the Fe interface. Further support to this idea is gained from the increase of the out-of-plane cell parameter of the LSMO layer detected by high-resolution x-ray diffraction in annealed samples (data not shown). On the other hand, the permeability of the MgO barrier for oxygen is also evidenced by the substantial reduction of the LSMO Curie temperature in MgO-capped LSMO layers. These results impose serious constraints on the growth process of Fe/MgO/LSMO heterostructures intended for the implementation of high-TMR-response MTJs.

I - V curves measured by sweeping voltage are nonlinear (as shown in the inset of Fig. 3), and the conductance of the junctions as a function of bias voltage is asymmetric and parabolic at low bias, thus suggesting tunneling transport. Particular attention was paid to the junction's zero-field resistance variations as a function of temperature that, according to the results reported in Ref. [26], provides information regarding the barrier quality and allows confirmation of tunneling conduction. Figure 3 depicts the temperature dependence of the resistance for an $18 \times 9 \mu\text{m}$ [2] LSMO/MgO/Fe annealed junction for several positive bias values, which shows an exponential increase of the resistance when temperature is lowered, in contrast to the weak insulating behavior expected for MTJs with direct tunneling [26]. This dependence suggests the existence of impurity-assisted conduction channels through the barrier [27]. In fact, the presence of some defects levels in the band gap of MgO due to intrinsic microstructural defects (vacancies, interstitial and interfacial states), which can provide conducting channels in the MgO layer, leading to the degradation of the barrier performances, has been stated previously [15,28,29]. However, as shown in Ref. [29], hopping across localized states in the MgO/Fe system would not lead to an exponential increase of the junction resistance; thus other contributions, such as increase of resistance at the LSMO topmost layers due to oxygen migration, and

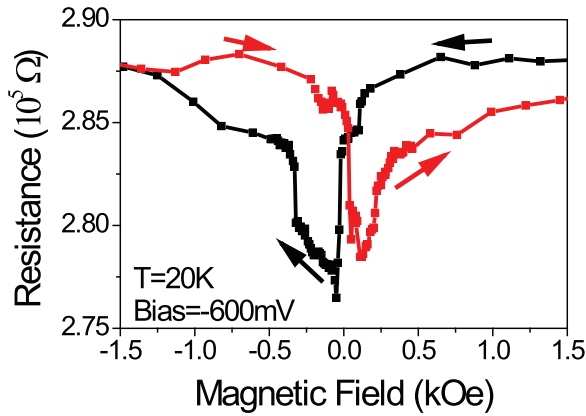


FIG. 4. (Color online) TMR response of a $5 \times 10 \mu\text{m}^2$ -sized Fe/MgO(2.4 nm)/LSMO nonannealed magnetic tunnel junction.

structural disorder with the appearance of FeO_x at the Fe/MgO interface, should also play a relevant role in this increase of the junction resistance. In principle a negative TMR response should be expected according to the negative and positive effective spin polarization of Fe/MgO interface and LSMO electrode, respectively. However, when electronic symmetries are taken into consideration, the sign of the TMR response is not so evident. Conduction electrons in LSMO have Δ_1 electronic symmetry and positive spin polarization. On the other hand, MgO promotes dominant transmission of electrons with Δ_1 electronic symmetry, and Δ_1 symmetry conduction electrons in bcc Fe have positive spin polarization. Accordingly, a spin-polarized Δ_1 transport channel should be the dominant conduction channel in this system and, consequently, an effective positive spin polarization at both interfaces should be expected. Therefore the TMR response of a LSMO/MgO/Fe system should be positive. In contrast, a negative TMR response is found in every range of temperatures (see Figs. 4, 5, and S3 [16]). These results make evident the relevance of structural disorder at the MgO/Fe interface in nonannealed samples that destroys the Δ_1 symmetry filtering effect and leads to a negative effective spin polarization of the Fe/MgO interface due to a complex density of states

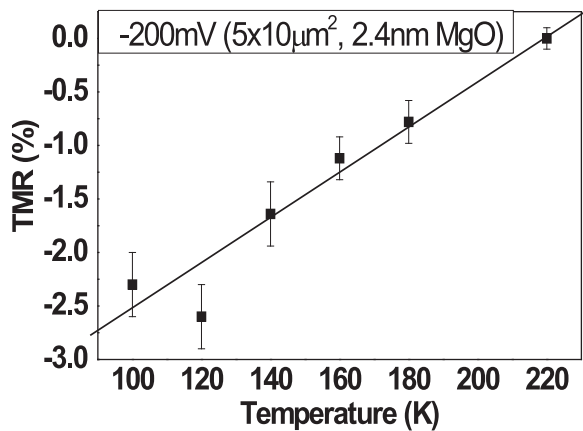


FIG. 5. Temperature dependence of the negative TMR (measured at -200 mV for the same junction as in Fig. 4). The line is a guide to the eyes.

at the Fe surface [13,30]. The switch from parallel (P) configuration to antiparallel (AP) configuration, which takes place at $H \sim 50 \text{ Oe}$ and results in a lower device resistance, is basically abrupt. However, the switch at higher field (from the antiparallel state to the parallel state) seems to take place in a two-step process: a relatively sharp switch at around 250–300 Oe and a gradual rotation of the electrodes to gain back the parallel configuration of electrodes. It is also worth mentioning that the resistance at the antiparallel state is not constant but tends to increase for higher fields, which could indicate a small misalignment between the applied field H and the easy axis of the electrodes, so that instead of viewing a single switch, a gradual rotation of the electrode's magnetization causes a variation in the resistance in the AP configuration. Minor loops make evident the switching of the magnetization of only one of the ferromagnetic electrodes, thus confirming the phenomenon is indeed TMR, in spite of its small value ($\text{TMR} \leq 4\%$) (see Fig. S3 from Supplemental Material [16]). The temperature dependence of the negative TMR response is plotted in Fig. 5. TMR decreases monotonically on increasing temperature and becomes vanishingly small at around $T \sim 200 \text{ K}$.

Possible strategies to improve the TMR response in this system involve achieving sharp clean Fe/MgO interfaces restoring symmetry filtering effect, and stoichiometric MgO barriers. In this sense, in Fe/MgO/Fe MTJs the use of thermal annealing and incorporation of a thin $\sim 5 \text{ \AA}$ Mg layer into the barrier/electrode interface have shown to be effective. Either improvement of (001) texture in the MgO layer or improvement of interface sharpness and reduction of interfacial oxides are routinely suggested [31]. Nevertheless, the reason of this effectiveness is still unclear. On the other hand, strain-induced changes of local symmetry at the LSMO/barrier interface may promote weak changes on the local Mn valence [32] that could further degrade the TMR response. This latter effect may be partially compensated by modulating the interface doping profile in a similar way to the approach reported by Yamada and co-workers [33].

Annealing the samples improves the structural quality at the Fe/MgO interface, leading eventually to the formation of an ordered oxide layer (see Fig. 1). The TMR response in annealed samples exhibits a positive abrupt switch between two resistance states at temperatures below about 120 K [see Fig. 6(a)]. For higher temperatures [see Fig. 6(b)], TMR curves evidence the superposition of positive and negative contributions and, as temperature further increases [Fig. 6(c)], only the negative TMR contribution remains. As mentioned above, in optimal conditions with clean epitaxial MgO/Fe interfaces, a spin-polarized Δ_1 transport channel should be the dominant conduction channel in the LSMO/MgO/Fe system, leading to a positive TMR response. However, XPS spectra clearly show an increase of the FeO_x at the Fe/MgO in annealed samples (see Fig. S2 [16]); thus the positive TMR response observed in those samples cannot be attributed to a symmetry filtering effect at the MgO/Fe interface. The presence of an iron oxide layer would add more complexity to the electronic structure of the interface, enabling the suppression or even the sign reversal of the TMR response by temperature changes or by appropriate bias polarity [8,29,30]. In fact, recent reports have shown that an inversion of the spin polarization occurs at oxidized interfaces due to $3d$ - $2p$ hybridization. It has

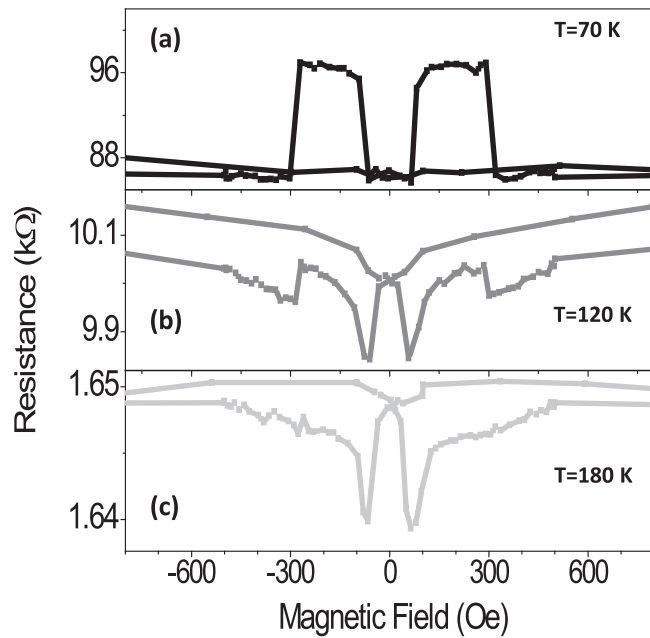


FIG. 6. Dependence of magnetoresistance on the applied magnetic field at a fixed applied voltage bias of 100 mV and different temperatures for an annealed junction of $9 \times 18 \mu\text{m}^2$ and MgO thickness of 2.4 nm. (a) At 70 K, a positive TMR with well-defined antiparallel magnetizations of both LSMO and Fe electrodes is observed. (b) At 120 K, the TMR is mainly negative but a visible positive contribution persists. (c) At higher temperatures, only the negative magnetoresistance remains.

been theoretically demonstrated that the larger population of majority antibonding orbitals (as compared to the minority ones) has a spin-filtering effect, causing a positive spin polarization of the tunneling current [13].

The positive TMR ratio increases in amplitude with decreasing temperature and reaches $\sim +25\%$ at 10 mV at around $T = 70$ K (see Fig. S5 from the Supplemental Material [16]). The positive TMR was also found to decrease with bias voltage (see Fig. 7), which is a quite common behavior in magnetic tunnel junctions, as discussed by Tsymbal *et al.* [34].

In this scenario, the complex temperature dependence of the TMR would result from the competing negative contribution of the (bulklike) electrodes and the temperature-dependent spin-filtering effect of the FeO_x interfacial layer. The fact that the change in sign of the TMR signal occurs around $T \sim 120$ K, together with the upward shift of the binding energy peak as we approach the interface with MgO (see Fig. 2), strongly suggest that the interfacial iron oxide layer would be mostly Fe_3O_4 . The loss of spin filtering would be related to the Verwey transition (expected around 120 K) in which Fe_3O_4 goes from insulator to semiconductor. In fact, previous works on Fe/MgO core-shell nanoparticles yielded a change of sign of MR at the same temperature and Fe_3O_4 was observed at the interface [35]. In our junctions, at low temperatures the interfacial oxide induces the depolarization of the tunneling current, besides the spin filtering, yielding the modest positive TMR. The switching fields therefore correspond to the LSMO coercive field and to that of the Fe exchange coupled with the FeO_x layer, and so are considerably large [~ 300 Oe, from

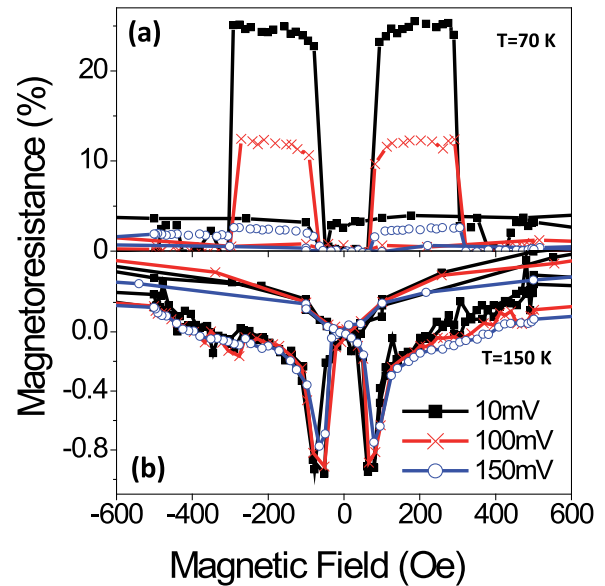


FIG. 7. (Color online) Dependence of magnetoresistance on the applied bias voltage for an annealed junction of $9 \times 18 \mu\text{m}^2$ and MgO thickness of 2.4 nm. (a) At 70 K, the positive TMR notably decreases with increasing voltage bias. (b) At 150 K, the negative contribution is rather insensitive to changes of the voltage bias.

Fig. 7(a)]. At higher temperatures, however, the interfacial oxide is no longer insulating, so it does not filter and the TMR takes negative values as in nonannealed samples.

It is worth mentioning that, in addition to Fe oxidation at the interface, the existence of oxygen vacancies within the MgO barrier itself [29,36], structural defects [37], and roughness [38] may also influence the interfacial electronic structure and therefore contribute to modify the TMR response. The particular case of oxygen vacancies has been deeply analyzed in Ref. [29], showing that they can alter the effective barrier height for symmetry-resolved charge carriers, leading to a decrease of the TMR response as temperature increases.

With the aim of reducing the resistance of the MTJs, we have also analyzed the dependence on the barrier thickness by narrowing the MgO layer down to 1.2 nm. As expected, this results in lower resistance values, which enable less noisy data at low T . In addition, smaller voltage bias dependence of TMR was found. However, maximum TMR response was reduced and values hardly above 10% were found (see Fig. S6 in Supplemental Material [16]). The reduction of the TMR values are explained because for thin barriers electrons with momentum vectors deviating from the barrier-normal direction have a finite tunneling probability that decreases both the spin polarization and the MR ratio. (The $\text{Fe}-\Delta_1$ band has its highest spin polarization in the barrier-normal ([001]) direction [8]). In addition, thinner MgO barriers would favor Fe oxidation driven by the oxygen transfer from the LSMO layer. This fact could strongly modify the quality and oxidation degree of the FeO_x layer and therefore affect its electronic properties.

On the other hand, the reduction of the MgO barrier thickness entails the appearance of AF coupling between the LSMO electrode and the FeO_x layer, as can be inferred from the behavior observed in some minor loops (see Fig. S7 from the Supplemental Material [16]). Due to the competition

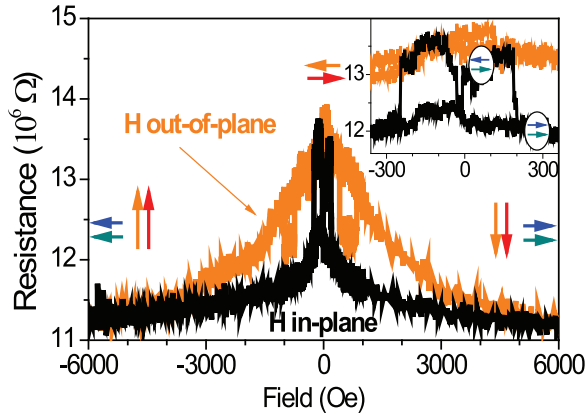


FIG. 8. (Color online) Dependence of the magnetoresistance on the direction of the applied magnetic field for a fixed applied voltage bias of -50 mV at $T = 10$ K [$5 \times 15 \mu\text{m}^2$ junction from an Fe (20 nm)/MgO(1.2 nm)/(42) LSMO stack]. The magnetic field was applied parallel to the surface, along the [100] Fe easy axis (H in-plane) and perpendicular to the film (H out-of-plane). Inset shows zoom for lower magnetic fields, for clarity.

between AF interaction, which gives rise to a sort of exchange bias field, and the coercive field, switching from P to AP configuration, takes place before crossing $H = 0$; concomitantly, the switching back to P configuration takes place at larger H than expected (~ 400 Oe), because the system needs more energy to overcome the effect of the AF coupling. The effect of this AF coupling can be also appreciated in TMR measurements with the magnetic field H applied out of plane, i.e., perpendicular to the junction plane (see Fig. 8). For large fields, the magnetizations of the electrodes are parallel to each other and aligned along H , and the low measured resistance coincides for both in-plane and out-of-plane configurations (R_P in Fig. 8). However, as shown in the inset of Fig. 8, the resistance obtained at low fields for H out-of-plane configuration coincides with the resistance measured for the antiparallel alignment of magnetizations, in the case of the H in-plane configuration (R_{AP} in Fig. 8). This suggests that a rotation of the magnetic moment of the electrodes takes place to favor antiparallel alignment at $H = 0$.

In addition, for the out-of-plane configuration, a switching towards lower resistance (which yields an intermediate value of resistance between the R_{AP} and R_P) occurs at fields above 400 Oe. We surmise that this negative TMR is a 90° configuration between magnetizations, which may result from the competition between the alignment of the magnetization of the electrodes along the externally applied magnetic field, the in-plane anisotropy of thin films, and the AF coupling. It is worth mentioning here that perpendicular magnetic anisotropy has been reported, both theoretically and experimentally, in the Fe/MgO system [39], but it has also been shown that it strongly depends on the oxidation degree of interfaces [40,41]. In addition, AF coupling due to interlayer exchange coupling has also been reported for the Fe/MgO/Fe system for MgO barrier thicknesses around 1 nm [42]. Furthermore, some theoretical studies also predict AF coupling for MgO barrier thicknesses below about 2 nm and in close correlation with its structural quality (defects, oxygen vacancies, etc.) [43],

therefore in good agreement with the results shown here. It is important to signal that this behavior opens the door to the design of three resistance-state devices.

IV. CONCLUSIONS

Our work emphasizes the relevant role of interfaces in the final response of magnetic tunneling junctions and evidences that appropriate interface engineering will allow controlling the final behavior of the system. In optimal conditions the LSMO/MgO/Fe system should exhibit a positive TMR response because the spin-polarized Δ_1 transport channel should be the dominant conduction channel and effective positive spin polarization at both interfaces should be expected. However, negative TMR response is observed in nonannealed samples due to structural disorder with the presence of FeO_x by the Fe/MgO interface that suppresses the symmetry filtering effect. Our results show that by properly modifying Fe/MgO interface, a positive TMR response of about 25% at 70 K can be obtained. However, this positive TMR is most likely to result from modified bonding at the interface between the Fe electrode and the MgO barrier due to improvement of microstructural quality, leading eventually to the formation of an ordered FeO_x layer. The positive TMR becomes vanishingly small at about 120 K, and above this temperature only the small negative TMR response, as in nonannealed samples, is observed. This fact, together with the upward shift of the binding energy peak in the Fe $2p$ region in XPS spectra, strongly indicate that the interfacial iron oxide layer would be mostly Fe_3O_4 . The loss of spin filtering would be related to the Verwey transition (expected at $T_V \sim 120$ K) in which Fe_3O_4 goes from insulator below T_V to semiconductor. This FeO_x layer has been reported to form at the interface between Fe and MgO, even in high-vacuum conditions, due to Fe-O bonding [24]. Although in Fe/MgO/Fe systems the FeO_x layer is suppressed by appropriate annealing treatments, in our case an enhancement of the FeO_x layer after annealing is detected, thus suggesting that the LSMO layer may well act as an extra source of oxygen for the oxidation of the Fe interface. While our results envisage the possibility of integrating half-metal electrodes with spin-filtering barriers, it also makes evident the intrinsic difficulties in combining transition-metal oxides with metals such as Fe or Co. In addition, an effort is necessary to improve the crystal quality at the interface, which should lead to higher TMR values and possibly also to larger spin selectivity by the barrier.

ACKNOWLEDGMENTS

We acknowledge financial support from the Spanish MINECO through grants (MAT2012-33207, MAT2011-27470-C02, MAT2012-37638 and Consolider Ingenio 2010 - CSD2009-00013 (Imagine)), from CAM through Grant No. S2009/MAT-1756 (Phama) and Basque Government (PI2011-1). Financial support from EC through FEDER program and Marie Curie Actions (256470-ITAMOSCINOM) is also acknowledged. C.M.B. thanks the Spanish MINECO for the financial support through the RyC program. The authors would like to thank the technical staff of the ICMAB for their assistance.

- [1] M. Jullière, *Phys. Lett. A* **54**, 225 (1975).
- [2] M. Bowen, M. Bibes, A. Barthélémy, J.-P. Contour, A. Anane, Y. Lemaître, and A. Fert, *Appl. Phys. Lett.* **82**, 233 (2003).
- [3] J. P. Webster, *J. Phys. Chem. Solids* **32**, 1221 (1971).
- [4] M. Bowen, A. Barthélémy, V. Bellini, M. Bibes, P. Seneor, E. Jacquet, J.-P. Contour, and P. H. Dederichs, *Phys. Rev. B* **73**, 140408(R) (2006).
- [5] M. Bowen, J.-L. Maurice, A. Barthélémy, P. Prod'homme, E. Jacquet, J. P. Contour, D. Imhoff, and C. Colliex, *Appl. Phys. Lett.* **89**, 103517 (2006).
- [6] Z. Sefrioui, C. Visani, M. J. Calderón, K. March, C. Carrétéro, M. Walls, A. Rivera-Calzada, C. León, R. Lopez Anton, T. R. Charlton, F. A. Cuellar, E. Iborra, F. Ott, D. Imhoff, L. Brey, M. Bibes, J. Santamaria, and A. Barthélémy, *Adv. Mater.* **22**, 5029 (2010); F. A. Cuellar, Y. H. Liu, J. Salafranca, N. Nemes, E. Iborra, G. Sanchez-Santolino, M. Varela, M. Garcia Hernandez, J. W. Freeland, M. Zhernenkov, M. R. Fitzsimmons, S. Okamoto, S. J. Pennycook, M. Bibes, A. Barthélémy, S.G.E. te Velthuis, Z. Sefrioui, C. Leon, and J. Santamaria, *Nat. Commun.* **5**, 4215 (2014).
- [7] M. Bowen, V. Cros, F. Petroff, A. Fert, C. Martínez-Boubeta, J. L. Costa-Krämer, J. V. Anguita, A. Cebollada, F. Briones, J. M. de Teresa, L. Morellón, M. R. Ibarra, F. Güell, F. Peiró, and A. Cornet, *Appl. Phys. Lett.* **79**, 1655 (2001).
- [8] S. Yuasa, T. Nagahama, A. Fukushima, Y. Suzuki, and K. Ando, *Nat. Mater.* **3**, 868 (2004).
- [9] S. S. P. Parkin, C. Kaiser, A. Panchula, P. M. Rice, B. Hughes, M. Samant, and S. H. Yang, *Nat. Mater.* **3**, 862 (2004).
- [10] A. Bhattacharya, S. J. May, S. G. E. te Velthuis, M. Warusawithana, X. Zhai, B. Jiang, J. M. Zuo, M. R. Fitzsimmons, S. D. Bader, and J. N. Eckstein, *Phys. Rev. Lett.* **100**, 257203 (2008).
- [11] Yaohua Liu, F. A. Cuellar, Z. Sefrioui, J. W. Freeland, M. R. Fitzsimmons, C. Leon, J. Santamaria, and S. G. E. te Velthuis, *Phys. Rev. Lett.* **111**, 247203 (2013).
- [12] X. Wu, Z. Zhang, and J. Meng, *Appl. Phys. Lett.* **100**, 122408 (2012).
- [13] E. Yu. Tsymbal, I. I. Oleinik, and D. G. Pettifor, *J. Appl. Phys.* **87**, 5230 (2000); K. D. Belashchenko, E. Y. Tsymbal, M. van Schilfhaarde, D. A. Stewart, I. I. Oleinik, and S. S. Jaswal, *Phys. Rev. B* **69**, 174408 (2004).
- [14] E. J. W. Verwey, *Nature (London)* **144**, 327 (1939).
- [15] C. Martínez-Boubeta, Z. Konstantinović, Ll. Balcells, S. Estradé, J. Arbiol, A. Cebollada, and B. Martínez, *Cryst. Growth Des.* **10**, 1017 (2010).
- [16] See Supplemental Material at <http://link.aps.org/supplemental/10.1103/PhysRevB.92.094428> for figures including Sketch of the LSMO/MgO/Fe stacking sequence, XPS data and different TMR data and its temperature dependence are provided.
- [17] D. Telesca, B. Sinkovic, S.-H. Yang, and S. S. P. Parkin, *J. Electron. Spectrosc. Relat. Phenom.* **185**, 133 (2012).
- [18] J. Schmalhorst, A. Thomas, G. Reiss, X. Kou, and E. Arenholz, *J. Appl. Phys.* **102**, 053907 (2007).
- [19] V. Serin, S. Andrieu, R. Serra, F. Bonell, C. Tiusan, L. Calmels, M. Varela, S. J. Pennycook, E. Snoeck, M. Walls, and C. Colliex, *Phys. Rev. B* **79**, 144413 (2009).
- [20] S. G. Wang, G. Han, G. H. Yu, Y. Jiang, C. Wang, A. Kohn, and R. C. C. Ward, *J. Magn. Magn. Mater.* **310**, 1935 (2007).
- [21] Y. Jang, C. Nam, K.-S. Lee, and B. K. Cho, *Appl. Phys. Lett.* **91**, 102104 (2007).
- [22] A. N. Chiamonti, D. K. Schreiber, W. F. Egelhoff, D. N. Seidman, and A. K. Petford, *Appl. Phys. Lett.* **93**, 103113 (2008).
- [23] R. B. Gangineni, C. Bellouard, A. Duluard, B. Negulescu, C. Baraduc, G. Gaudin, and C. Tiusan, *Appl. Phys. Lett.* **104**, 182402 (2014).
- [24] Y. Fan, K. J. Smith, G. Lüpke, A. T. Hanbicki, R. Goswami, C. H. Li, H. B. Zhao, and B. T. Jonker, *Nature Nanotechnol.* **8**, 438 (2013).
- [25] S. Pinitsoontorn, A. Cerezo, A. K. Petford-Long, D. Mauri, L. Folks, and M. J. Carey, *Appl. Phys. Lett.* **93**, 071901 (2008).
- [26] B. J. Jönsson-Åkerman, R. Escudero, C. Leighton, S. Kim, Ivan K. Schuller, and D. A. Rabson, *Appl. Phys. Lett.* **77**, 1870 (2000).
- [27] O. Txoperena, Y. Song, L. Qing, M. Gobbi, L. E. Hueso, H. Dery, and F. Casanova, *Phys. Rev. Lett.* **113**, 146601 (2014).
- [28] J. Zhang and L. D. Zhang, *Chin. Phys. Lett.* **363**, 293 (2002).
- [29] F. Schleicher, U. Halisdemir, D. Lacour, M. Gallart, S. Boukari, G. Schmerber, V. Davesne, P. Panissod, D. Halley, H. Majjad, Y. Henry, B. Leconte, A. Boulard, D. Spor, N. Beyer, C. Kieber, E. Sternitzky, O. Cregut, M. Ziegler, F. Montaigne *et al.*, *Nat. Commun.* **5**, 4547 (2014).
- [30] C. Tiusan, J. Faure-Vincent, C. Bellouard, M. Hehn, E. Jouguelet, and A. Schuhl, *Phys. Rev. Lett.* **93**, 106602 (2004).
- [31] A. T. Hindmarch, V. Harnchana, D. Ciudad, E. Negusse, D. A. Arena, A. P. Brown, R. M. D. Brydson, and C. H. Marrows, *Appl. Phys. Lett.* **97**, 252502 (2010).
- [32] S. Valencia, Z. Konstantinovic, D. Schmitz, A. Gaupp, Ll. Balcells, and B. Martínez, *Phys. Rev. B* **84**, 024413 (2011).
- [33] H. Yamada, Y. Ogawa, Y. Ishii, H. Sato, M. Kawasaki, H. Akoh, and Y. Tokura, *Science* **305**, 646 (2004).
- [34] E. Y. Tsymbal, O. N. Mryasov, and P. R. LeClair, *J. Phys.: Condens. Matter* **15**, R109 (2003).
- [35] C. Martínez-Boubeta, Ll. Balcells, S. Valencia, D. Schmitz, C. Monty, and B. Martínez, *Appl. Phys. Lett.* **94**, 262507 (2009).
- [36] G. X. Miao, Y. J. Park, J. S. Moodera, M. Seibt, G. Eilers, and M. Müntenberg, *Phys. Rev. Lett.* **100**, 246803 (2008).
- [37] F. Bonell, S. Andrieu, C. Tiusan, F. Montaigne, E. Snoeck, B. Belhadji, L. Calmels, F. Bertran, P. Le Fevre, and A. Taleb-Ibrahimi, *Phys. Rev. B* **82**, 092405 (2010).
- [38] C. Wang, A. Kohn, S. G. Wang, L. Y. Chang, S.-Y. Choi, A. I. Kirkland, A. K. Petford-Long, and R. C. C. Ward, *Phys. Rev. B* **82**, 024428 (2010).
- [39] J. W. Koo, S. Mitani, T. T. Sasaki, H. Sukegawa, Z. C. Wen, T. Ohkubo, T. Niizeki, K. Inomata, and K. Hono, *Appl. Phys. Lett.* **103**, 192401 (2013).
- [40] H. X. Yang, M. Chshiev, B. Dieny, J. H. Lee, A. Manchon, and K. H. Shin, *Phys. Rev. B* **84**, 054401 (2011).
- [41] B. Rodmacq, S. Auffret, B. Dieny, S. Monso, and P. Boyer, *J. Appl. Phys.* **93**, 7513 (2003).
- [42] J. Faure-Vincent, C. Tiusan, C. Bellouard, E. Popova, M. Hehn, F. Montaigne, and A. Schuhl, *Phys. Rev. Lett.* **89**, 107206 (2002).
- [43] M. Ye. Zhuravlev, E. Y. Tsymbal, and A. V. Vedyayev, *Phys. Rev. Lett.* **94**, 026806 (2005).